

Supplementary Figures for

Relating teleseismic backprojection images to earthquake kinematics

Jiuxun Yin¹, Marine A. Denolle¹

¹*Department of Earth and Planetary Sciences, Harvard University, Cambridge, MA, USA*

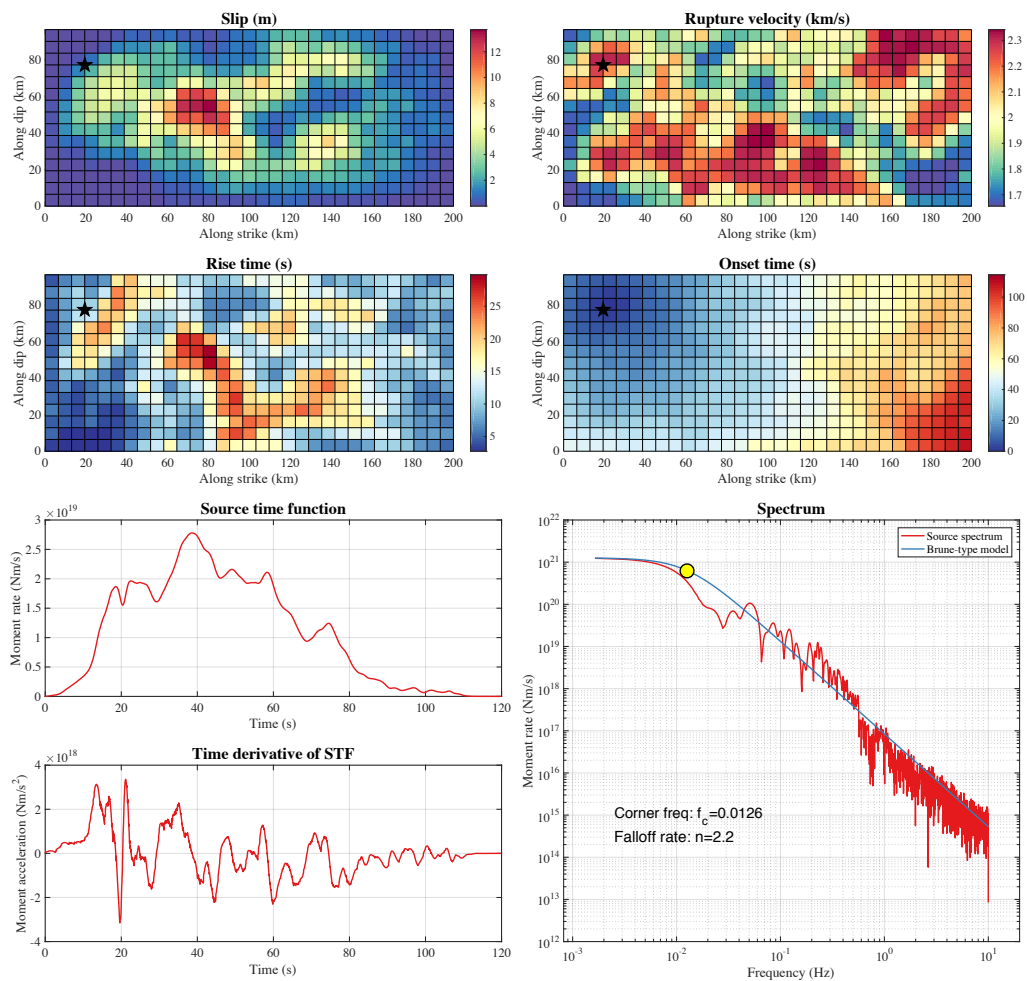


Figure S1. One example of the kinematic source used in this study and its relevant source parameters: (a) coseismic slip distribution; (b) rupture velocity distribution; (c) rise time distribution; (d) Onset time distribution; (e) moment rate function (source time function); (f) moment acceleration (time derivative of the source time function) and (g) source spectrum and the best-fit Brune type model.

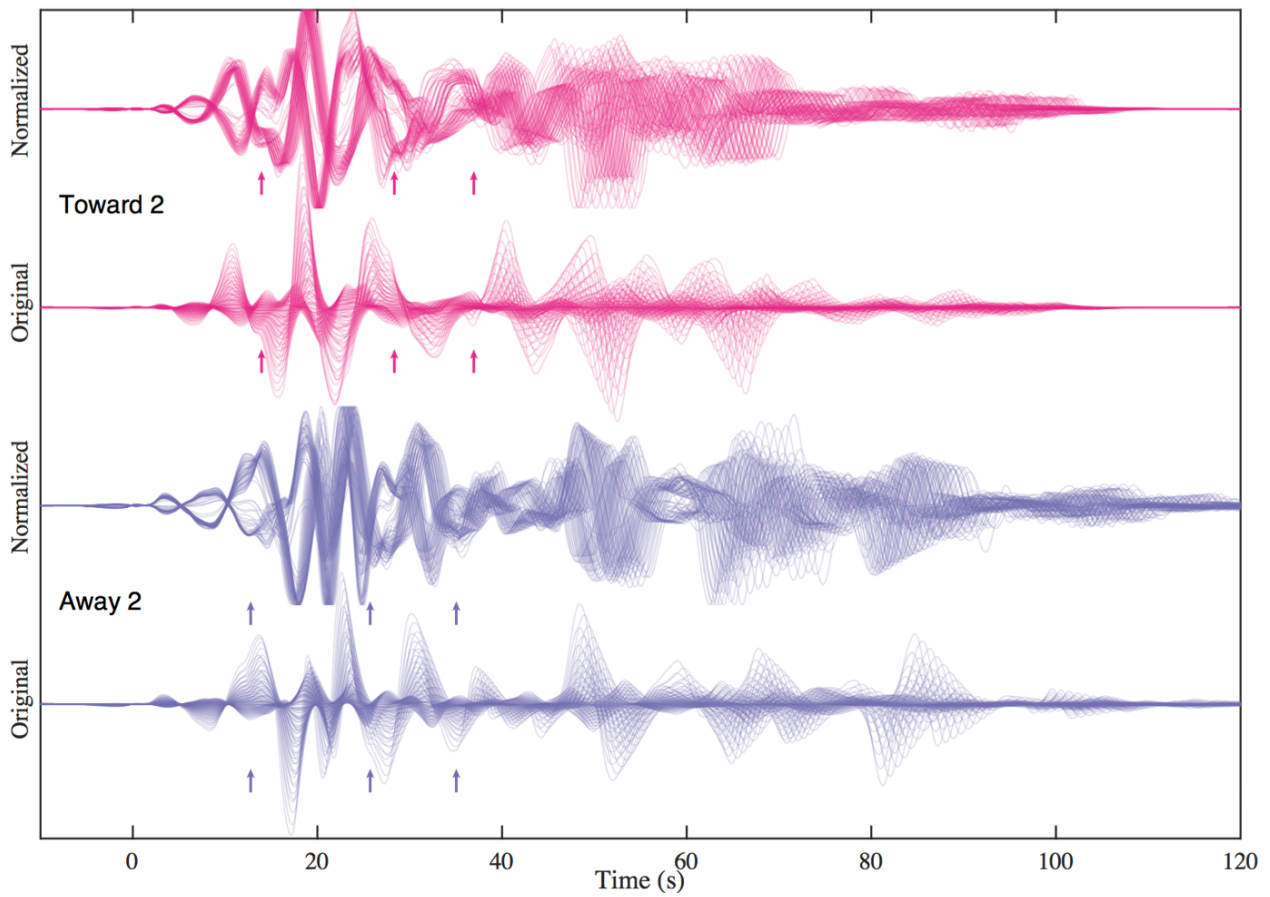


Figure S2. Waveforms recorded by the arrays near the nodal plane of focal mechanism (Toward2 and Away2 arrays). For each array, both the original waveforms (same as Fig.2 (b) in the main text) and the waveforms after amplitude normalization by their maxima are shown here. The normalized waveforms here more clearly indicate the secondary polarity flipping caused by rupture propagation, which is also highlighted by the arrows.

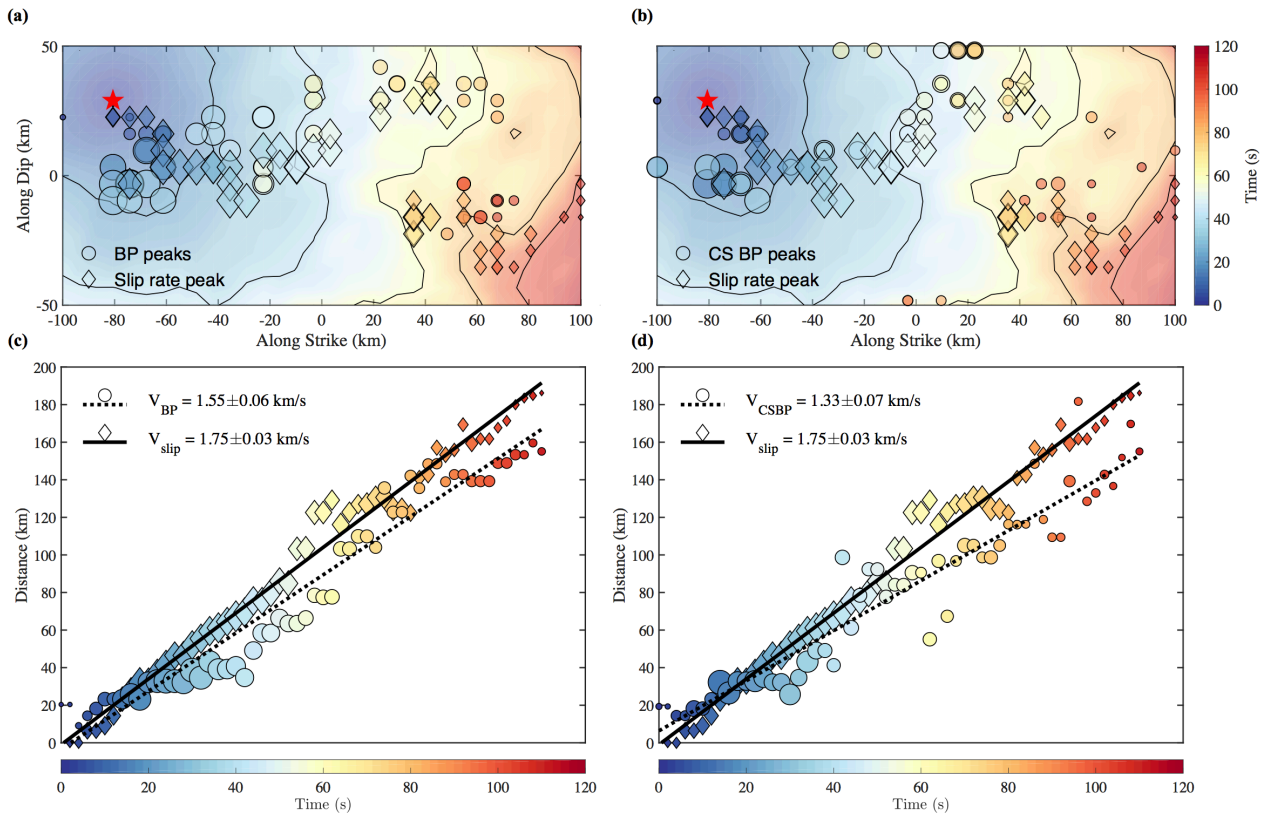


Figure S3. (a) Spatiotemporal evolution of Linear BP peaks (circles) from Away1 array compared with slip rate peaks (diamonds) and onset time distribution (background image) from the kinematic model. Color corresponds to both the peak time and onset time. Red star indicates the epicenter of the kinematic model. (b) same as (a) but for the CSBP peaks. (c) Distance from the BP peaks to the epicenter varying with time. The black bold line shows the linear fitting for the slip peaks while the black dashed line corresponds to the linear fitting for the BP peaks. Color of symbols and x-axis both indicate the peak time. (d) Same as (c) but for the CSBP peaks.

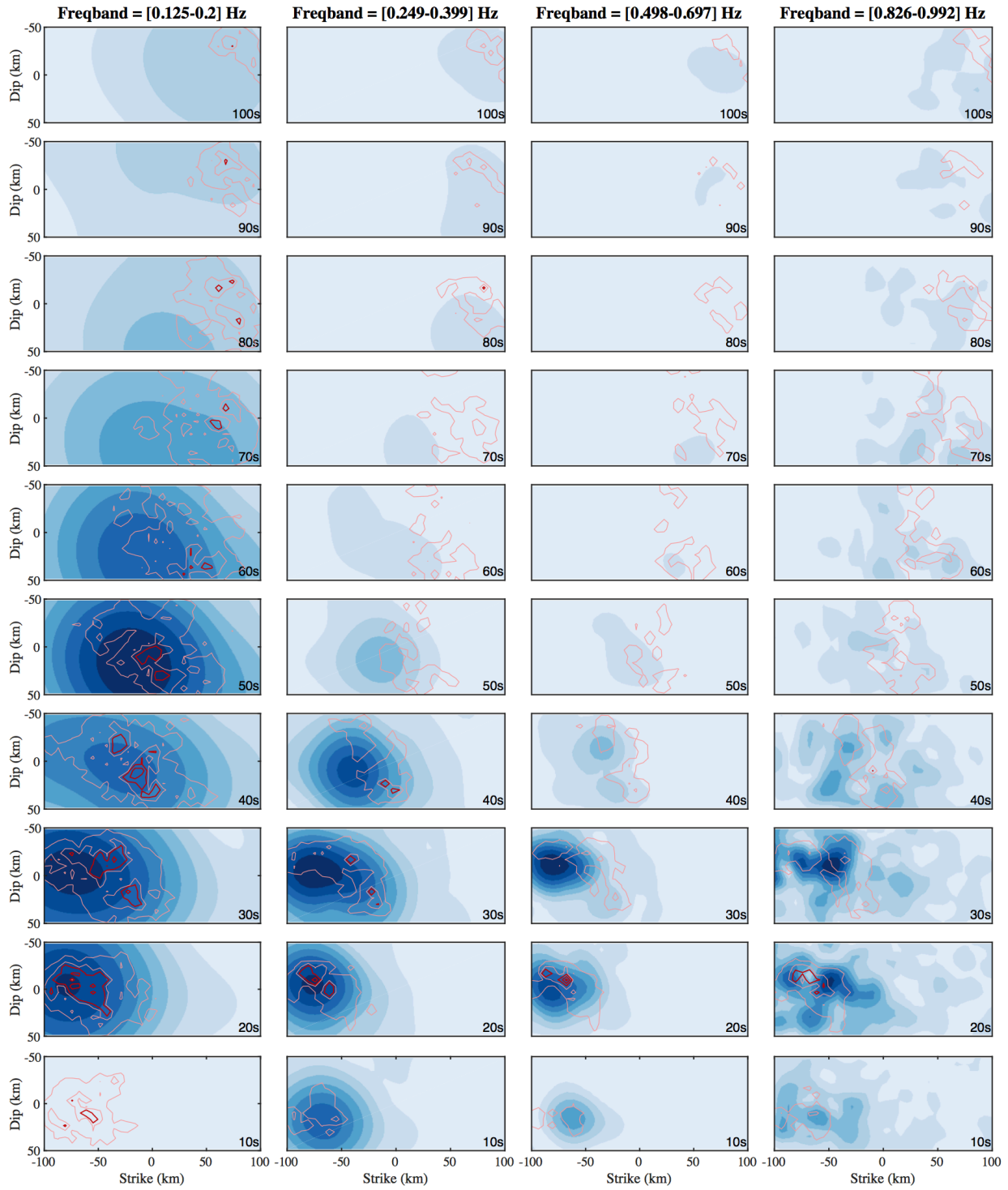


Figure S4. BP image (blue images) in each sub-frequency-band from Away1 array compared with the corresponding filtered slip rate distribution (red thick contours correspond to 10% of maximum amplitude while pink thin contours correspond to 1% of maximum amplitude) from the same kinematic source shown in Fig.3.

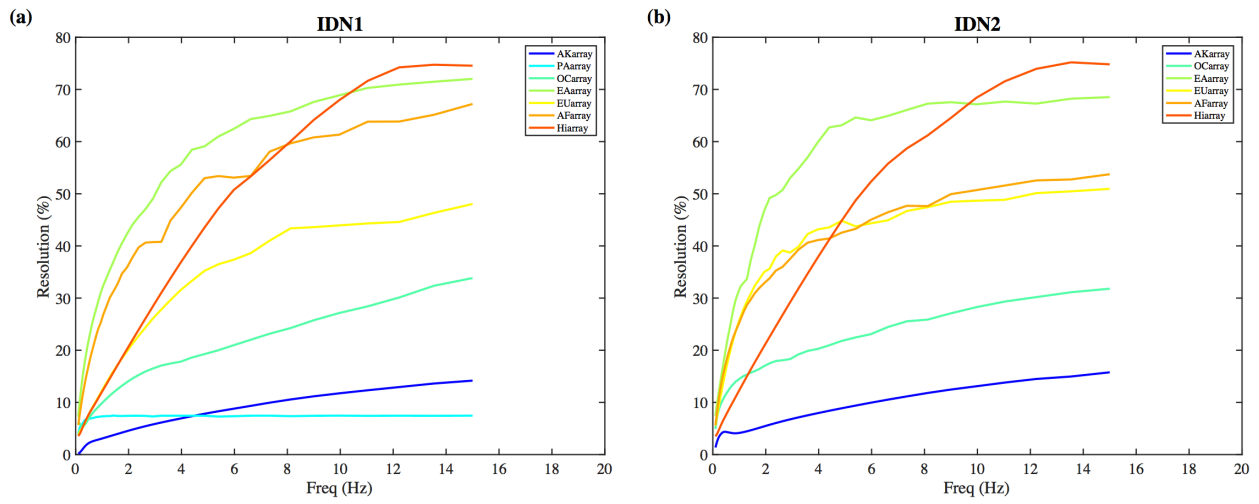


Figure S5. The variation of resolvability ϵ_r for all the available arrays within the teleseismic distance range to (a) IDN1 (Java) and (b) IDN2 (Sumatra) regions in a broad frequency band from 0.1 to 15 Hz.

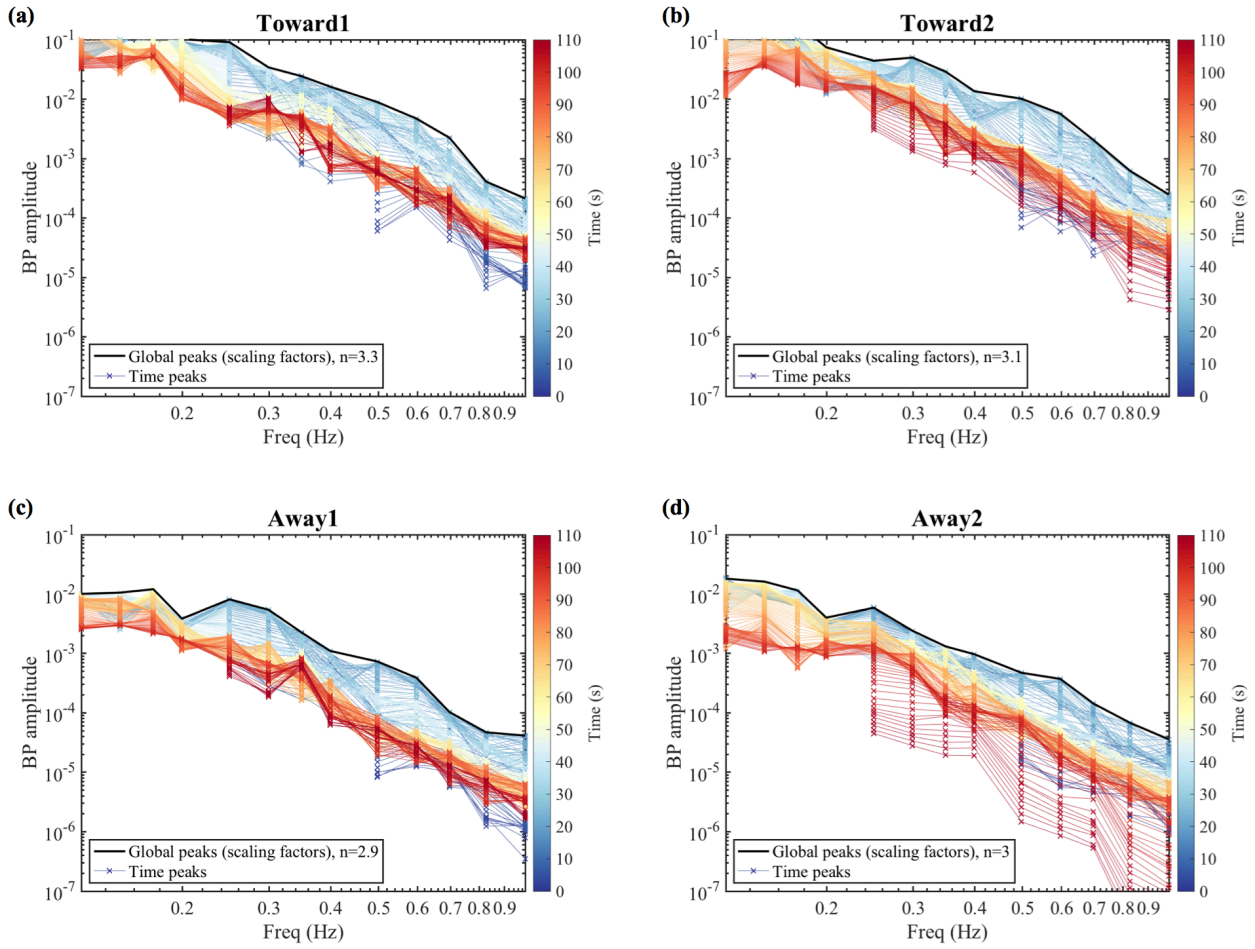


Figure S6. The spectral falloff of the BP peak amplitude for the kinematic source model from (a) Towards1 array; (b) Towards2 array; (c) Away1 array and (d) Away2 results. Crosse-lines show the BP peak amplitudes at the corresponding frequency in each time step that indicated by line colors. Black curves indicate the total BP peaks, which are used to normalized the BP images, during entire rupture at each frequency.

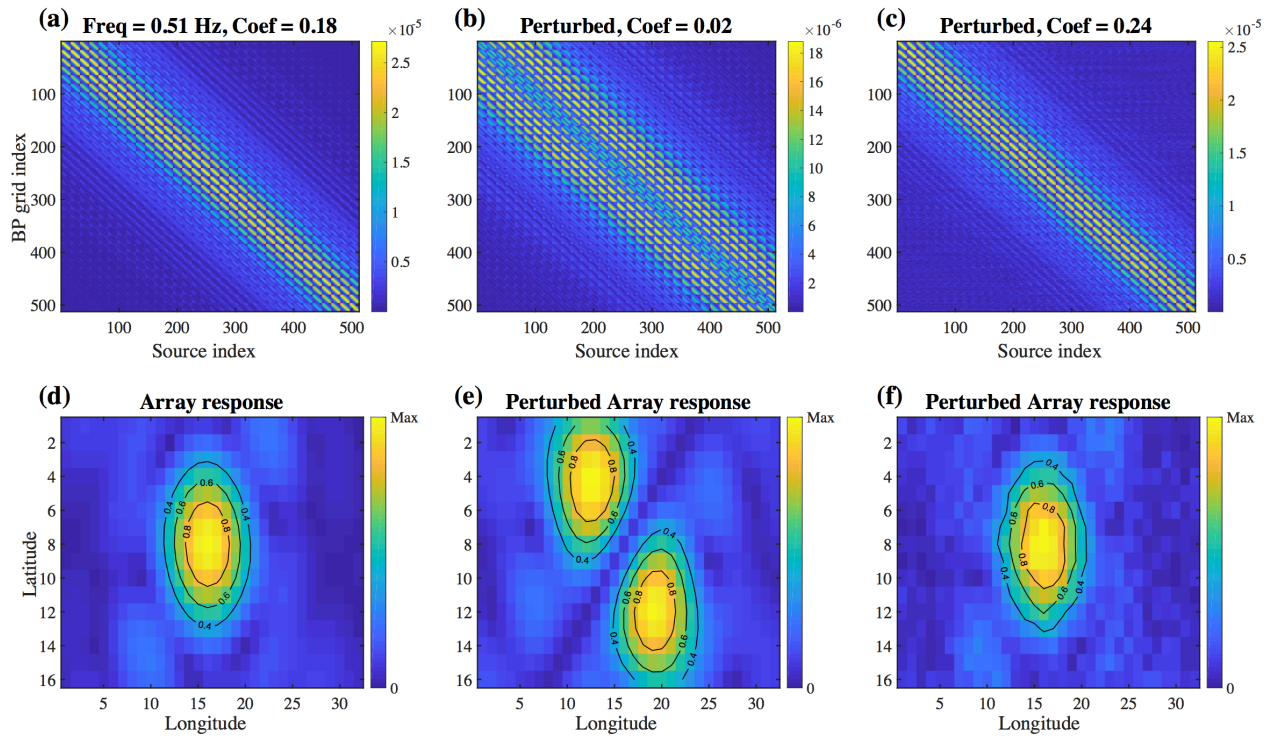


Figure S7. Calculated resolution matrices and their corresponding array response at the center (248th column of the resolution matrices): (a) and (d) from travel time without perturbation; (b) and (e) from systematically perturbed travel time; (c) and (f) from randomly perturbed travel time

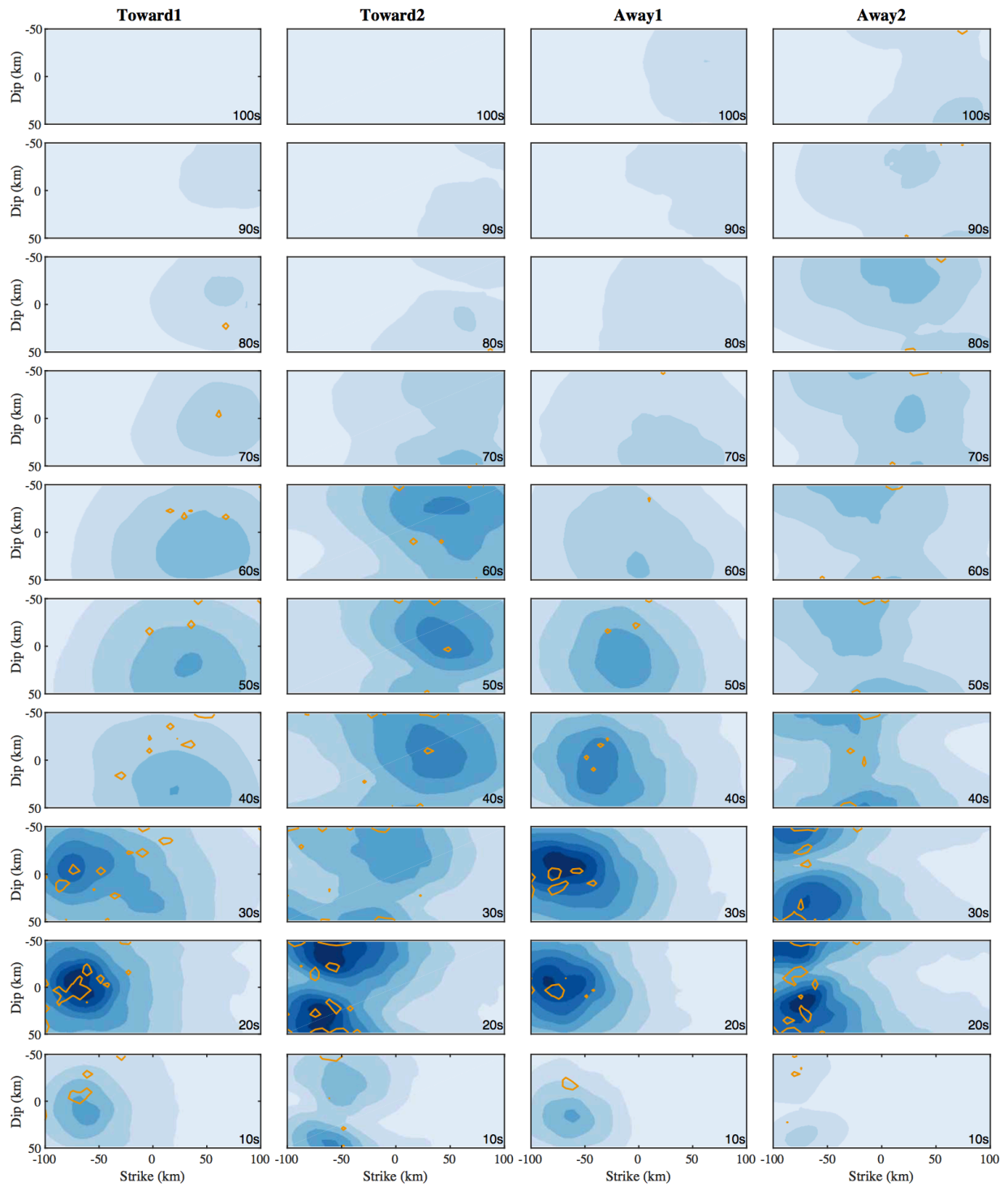


Figure S8. Comparison between the Linear BP image (blue images) with the CSBP results (yellow contours correspond to 20% of maximum CSBP amplitude) in each frequency band.

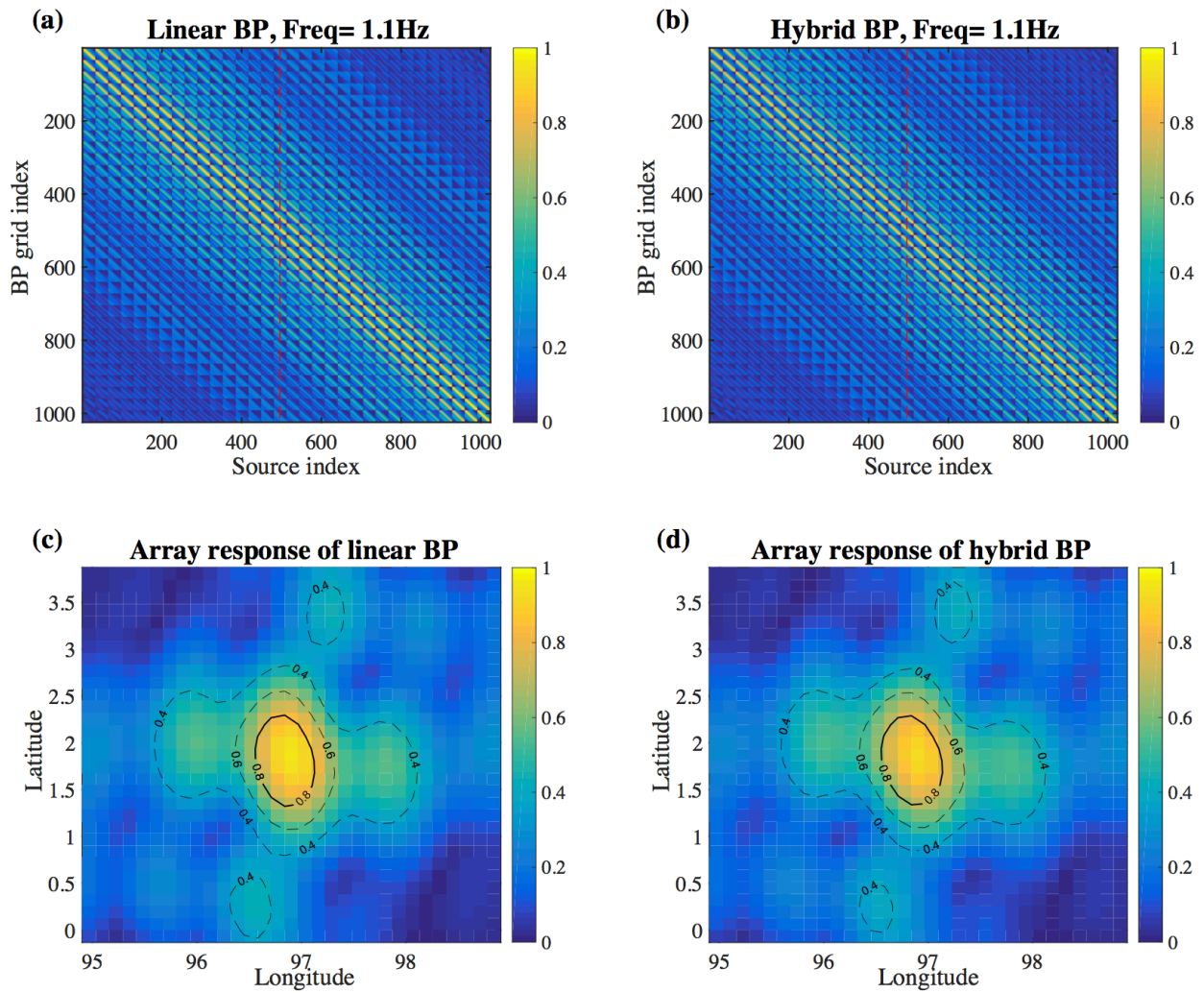


Figure S9. (a) Resolution matrix of the Hi-net array towards the IDN2 (Sumatra) region. It is same as that in Fig.1 (b) in the main text. (b) The corresponding resolution matrix calculated from the HyBP for the same configuration (Hi-net to IND2). Both resolution matrices are normalized to their maximum element. (c) and (d) show the corresponding array response at the same source location indicated by the red dashed lines in (a) and (b).